

Electronic supplementary information

A facile polymer mediated dye incorporation method for fluorescence encoded microbeads with large encoding capacities

Hajar Masoomi,[#] Yao Wang,^{#,*} Cang Chen, Jiayu Zhang, Yunfei Ge, Qingsheng Guo, Hongchen Gu, and Hong Xu^{*}

School of Biomedical Engineering, Shanghai Jiao Tong University, Shanghai, China

[#] These authors contributed equally to this work.

^{*}Corresponding authors.

E-mail: wangyao@sjtu.edu.cn (Y. Wang), xuhong@sjtu.edu.cn (H. Xu).

Experimental section

Materials. A series of mesoporous silica beads (MSBs, pore size of ~30 nm) with different diameters of 1.7, 3.3 and 5.5 μm (denoted as MSBs-1.7, MSBs-3.3 and MSBs-5.5, respectively), mesoporous polystyrene beads (MPSBs) with diameters of 2.9 μm (denoted as MPSBs-2.9, pore size of ~10 nm) and 5.5 μm (denoted as MPSBs-5.5, pore size of ~30 nm), and mesoporous polymethyl methacrylate beads (MPMBs, pore size of ~50 nm) with a diameter of 18.4 μm (denoted as MPMBs-18.4) were purchased from Suzhou Nanomicro Technology Co., Ltd., China. The carboxylated solid polystyrene beads with a diameter of 5.8 μm (denoted as SPSBs-5.8) were provided by Bangs Laboratories, USA. Poly(styrene-co-maleic anhydride) terminated with cumene (PSMA, $M_w = 1.7$ K) and poly(ethylenimine) (PEI, $M_w = 750$ K) were bought from Sigma-Aldrich. The beads of MPSBs-2.9 and MPSBs-5.5 were carboxylated by PSMA according to our previous work.¹ Fluorescein isothiocyanate isomer I (FITC, 96%) was gained from Aladdin Reagent (Shanghai) Co., Ltd. Rhodamine B isothiocyanate (RITC, 95%) was provided by Shanghai Dibai Biotechnology Co., Ltd., China. Carboxylated Fe_3O_4 magnetic nanoparticles (MNPs) were purchased from Shanghai So-Fe Biomedicine Co., Ltd., China. Ethanol (AR), *N,N*-Dimethylformamide (DMF, AR), tetraethyl orthosilicate (TEOS, AR), and ammonium hydroxide (AR) were bought from Sinopharm Chemical Reagent Co., Ltd., China. Millipore water (18.2 $\text{M}\Omega$ cm) was utilized in the preparation of all aqueous solutions.

Incorporation of dyes into mesoporous beads through the polymer mediated dye loading method. Firstly, the solution of FITC in ethanol (8 mg/mL, 0.54 mL) or RITC in DMF (22 mg/mL, 0.54 mL) was added into 15 mL of PEI aqueous solution (750 K, 10 mg/mL, 0.5 M NaCl, pH = 8.0) with a FITC: NH_2 mole ratio of 1:100 or a RITC: NH_2 mole ratio of 2:100. Then the mixture was shaken at 30 $^\circ\text{C}$ overnight by avoiding light to acquire dye-labeled PEI (FITC-PEI or RITC-PEI) solution. Thereafter, mesoporous beads with different particle number (6.4×10^8 for MSBs-1.7, 8×10^7 for MSBs-3.3 and MPSBs-2.9, 2×10^7 for MSBs-5.5, MPSBs-5.5 and SPSBs-5.8, and 6×10^5 for MPMBs-18.4) were ultrasonically suspended into 1.5 mL of a mixture containing FITC-PEI solution, RITC-PEI solution and blank PEI solution with different ratios and

rotationally reacted under darkness for 20 min. After being centrifugated and washed with water three times, the obtained dye-loaded beads were redispersed in 0.4 mL of aqueous solution.

Assembly of MNPs onto beads. In order to render the superparamagnetism to beads for rapid magnetic separation, the carboxyl groups functionalized MNPs were assembled onto aminated dye-loaded beads via electrostatic interactions. In detail, the aforementioned 0.4 mL of beads solution was dropwise added into 1.1 mL of MNPs aqueous solution (1 mg/mL) with ultrasonication. After a rotation of 30 min, the resultant beads were magnetically separated, followed by washing with water three times. Afterwards, the MNPs coated beads were added into 1.5 mL of PEI solution (750 K, 10 mg/mL, 0.5 M NaCl, pH = 8.0) to electrostatically adsorb another PEI layer under a rotation of 20 min and then washed with water three times. The aminated beads obtained herein were utilized for the next reactions.

Encapsulation of beads with a silica shell. In order to protect the incorporated dyes from leakage, the aforementioned beads were encapsulated with a silica shell to form the final fluorescence encoded microbeads (FEMs). Briefly, the aminated beads obtained in last step were washed with ethanol twice and introduced into a mixture containing 3 mL of ethanol, 300 μ L of water and 40 μ L of TEOS. After a pre-reaction of 30 min, 22 μ L of ammonium hydroxide was added and the system was further rotationally aged at 30 °C for 22 h. Then the products were washed with ethanol and water three times respectively to acquire the silica encapsulated FEMs.

Characterization. Fluorescent spectra of different samples were conducted on a F-2700 fluorescence spectrophotometer (HITACHI, Japan). Laser-scanning confocal images were recorded on a TCS SP5 confocal microscopy (Leica, Germany) with a laser of 488 nm as the excitation source and two emission channels (channel 1: 515 ± 15 nm, channel 2: 585 ± 15 nm) as detectors. The flow cytometry analyses were determined through an Accuri C6 instrument (BD, USA) by detecting forward scatter (FSC), side scatter (SSC), FL1 (515 ± 10 nm) and FL2 (565 ± 10 nm) channels with an excitation laser of 488 nm. The obtained data were further treated with an OPTICS clustering algorithm.² Considering the emission spectrum overlaps between FITC and RITC, the fluorescent compensation was used (FL2 was corrected by subtracting 10.3% of FL1, and FL1 was corrected by subtracting 1.9% of FL2). The particle number

counting of beads was acquired by flow cytometry on a NovoCyte 2040R instrument (ACEA, USA). Transmission electron microscopy (TEM) characterizations were performed on a JEM 2100F microscope (JEOL, Japan) operated at an accelerated voltage of 200 kV. To acquire the ultrathin sections of beads, the powder samples were passed through propylene oxide, infiltrated with EMbed 812 resin (Electron Microscopy Sciences, Hatfield, USA) overnight, cut with EM UC7 ultramicrotome (Leica, Germany) and then collected on copper grids. Scanning electron microscopy (SEM) images were obtained via a Zeiss Ultra Plus field emission scanning electron microscope (Carl Zeiss AG, Germany). Zeta potential measurements were carried out on a Zetasizer Nano instrument (Malvern, UK) at 298 K.

Supplementary Figures and Tables:

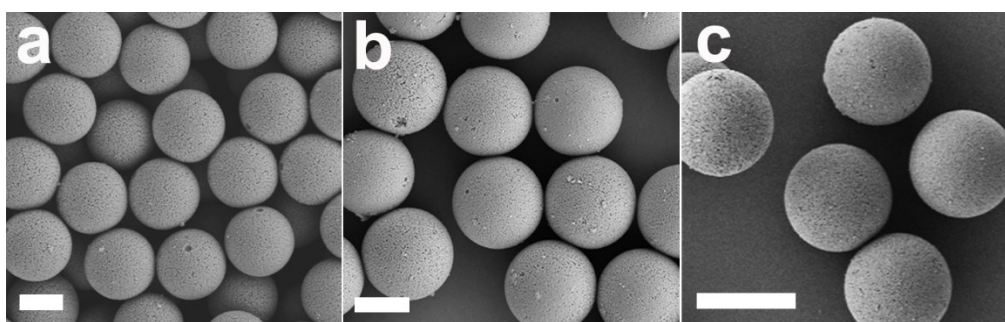


Figure S1. Representative SEM images of (a) MSBs-1.7, (b) MSBs-3.3 and (c) MSBs-5.5 at low magnification. Scale bar, (a) 1 μm , (b) 2 μm , (c) 5 μm .

Table S1. Size of different MSBs measured from their SEM images.

Sample name	Mean particle diameter	CV of particle diameter
	(μm)	(%)
MSBs-1.7	1.7	2.7
MSBs-3.3	3.3	2.9
MSBs-5.5	5.5	2.3

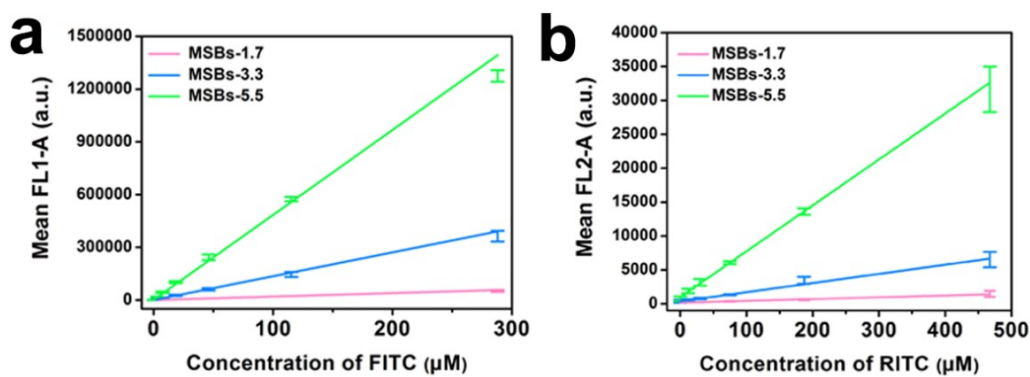


Figure S2. Relationship between fluorescent intensity of different FEMs obtained via flow cytometry and the concentration of dyes in the mixed PEI solution: (a) FITC in FL1 (515 ± 10 nm) channel and (b) RITC in FL2 (565 ± 10 nm) channel.

Table S2. Encoding formula of FEMs in FITC and RITC fluorescent intensity levels. MSBs-1.7: F0 and F5-F10 (FITC), R0 and R4-R5 (RITC); MSBs-3.3: F0 and F3-F10 (FITC), R0 and R3-R5 (RITC); MSBs-5.5: F0-F10 (FITC), R0-R5 (RITC).

FITC fluorescent intensity level	Volume of PEI solution		RITC fluorescent intensity level	Volume of PEI solution	
	Blank PEI (μ L)	FITC- PEI (μ L)		Blank PEI (μ L)	RITC- PEI (μ L)
F0	1500	0	R0	1500	0
F1	1499.6	0.4	R1	1467.7	32.3
F2	1499.0	1.0	R2	1419.4	80.6
F3	1497.5	2.5	R3	1298.4	201.6
F4	1493.9	6.1	R4	996	504
F5	1484.6	15.4	R5	240	1260
F6	1461.6	38.4			
F7	1404	96			
F8	1260	240			
F9	900	600			
F10	0	1500			

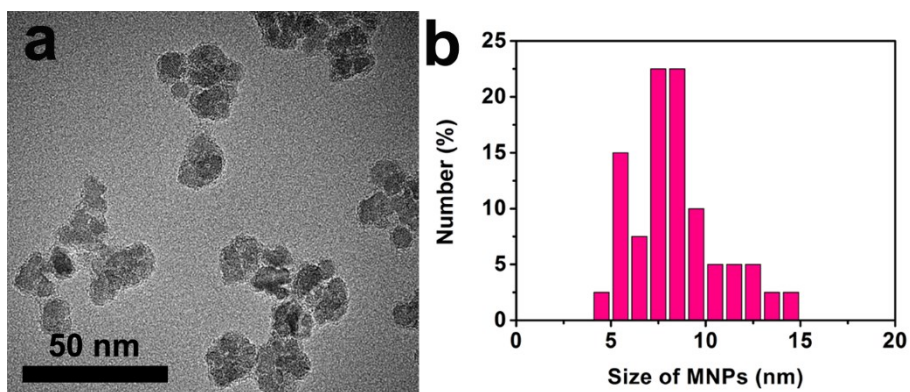


Figure S3. (a) TEM image of MNPs. (b) Particle size distribution of MNPs measured from their TEM images.

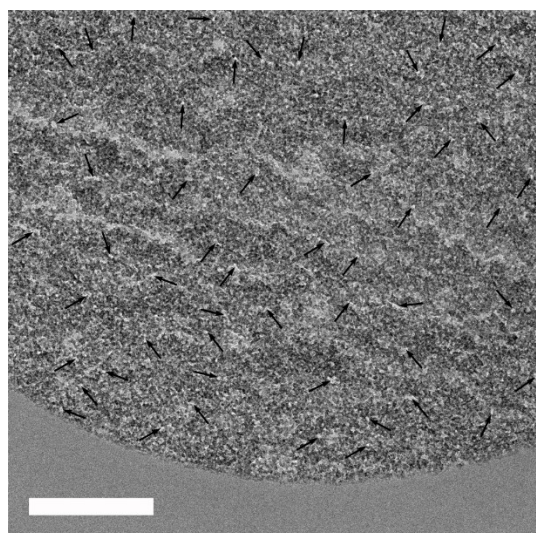


Figure S4. TEM image of the original MSBs-5.5 performed on their ultrathin sections (some mesopores are marked with black arrows). Scale bar, 500 nm.

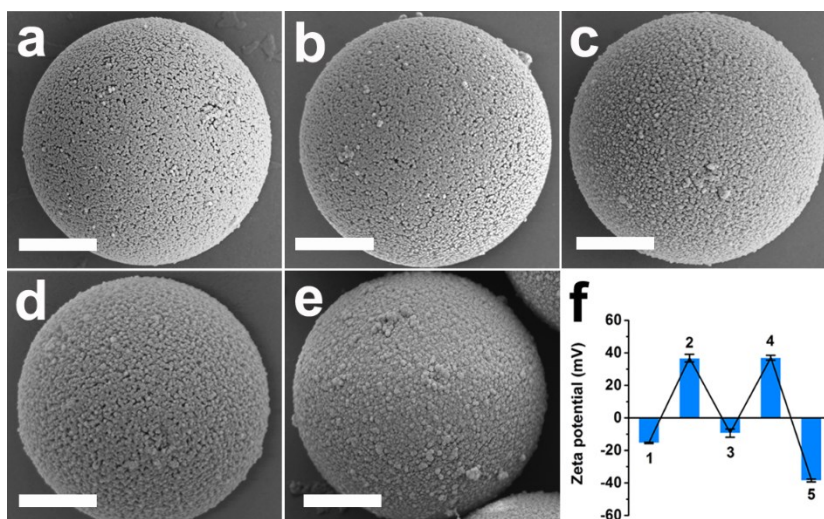


Figure S5. (a-e) High-magnification SEM images of MSBs-3.3 FEMs at different construction stages: (a) MSBs-3.3, (b) MSBs-3.3@dye, (c) MSBs-3.3@dye/MNPs, (d) MSBs-3.3@dye/MNPs/PEI, (e) MSBs-3.3@dye/MNPs/PEI/SiO₂ (namely the final MSBs-3.3 FEMs). Scale bar, 1 μ m. (f) Zeta potential values of various beads in aqueous solution. Samples of 1-5 correspond to a-e respectively.

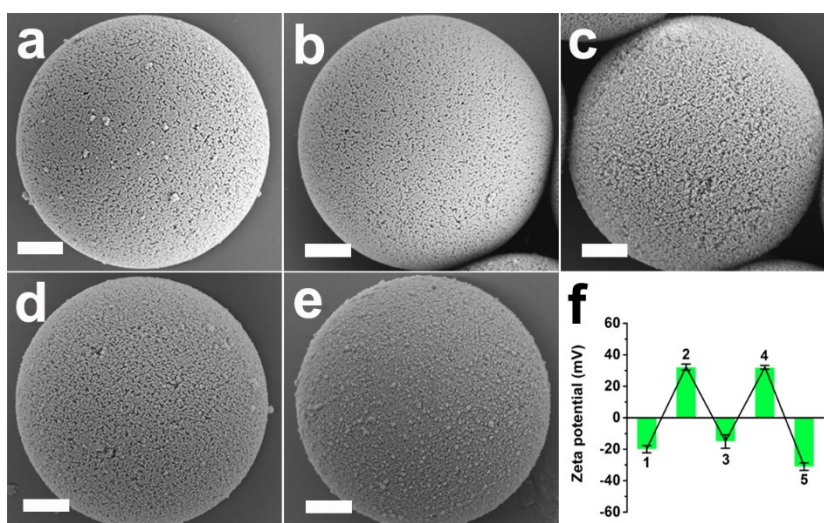


Figure S6. (a-e) High-magnification SEM images of MSBs-5.5 FEMs at different construction stages: (a) MSBs-5.5, (b) MSBs-5.5@dye, (c) MSBs-5.5@dye/MNPs, (d) MSBs-5.5@dye/MNPs/PEI, (e) MSBs-5.5@dye/MNPs/PEI/SiO₂ (namely the final MSBs-5.5 FEMs). Scale bar, 1 μ m. (f) Zeta potential values of various beads in aqueous solution. Samples of 1-5 correspond to a-e respectively.

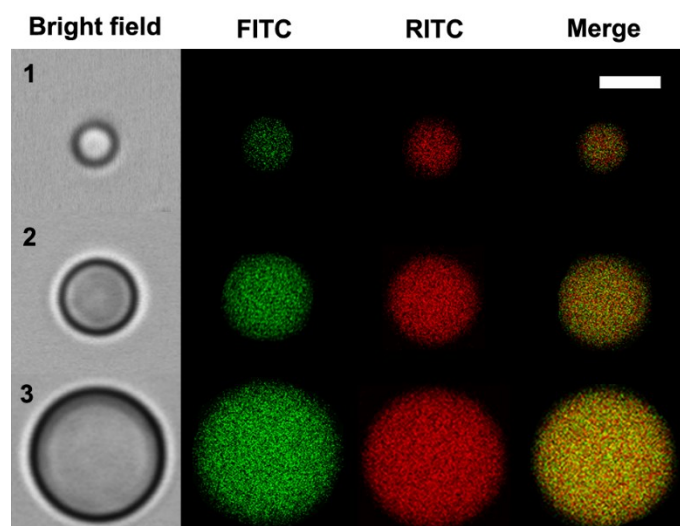


Figure S7. Confocal images of different dual dyes doped FEMs taken in bright field, channel 1 (515 ± 15 nm) for FITC, channel 2 (585 ± 15 nm) for RITC, and the merged ones of channel 1 and channel 2: (1) MSBs-1.7 FEMs, (2) MSBs-3.3 FEMs, (3) MSBs-5.5 FEMs. Scale bar, 2 μm .

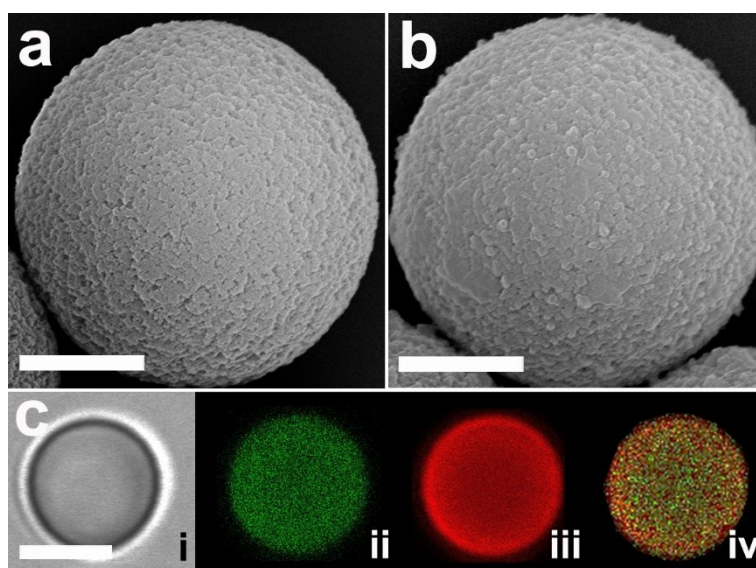


Figure S8. Representative SEM images of (a) original MPSBs-2.9 and (b) dual dyes doped MPSBs-2.9 FEMs at high magnification. (c) Confocal images of dual dyes doped MPSBs-2.9 FEMs taken in (i) bright field, (ii) channel 1 (515 ± 15 nm) for FITC, (iii) channel 2 (585 ± 15 nm) for RITC, and (iv) the merged one of channel 1 and channel 2. Scale bar, (a, b) 1 μm , (c) 2 μm .

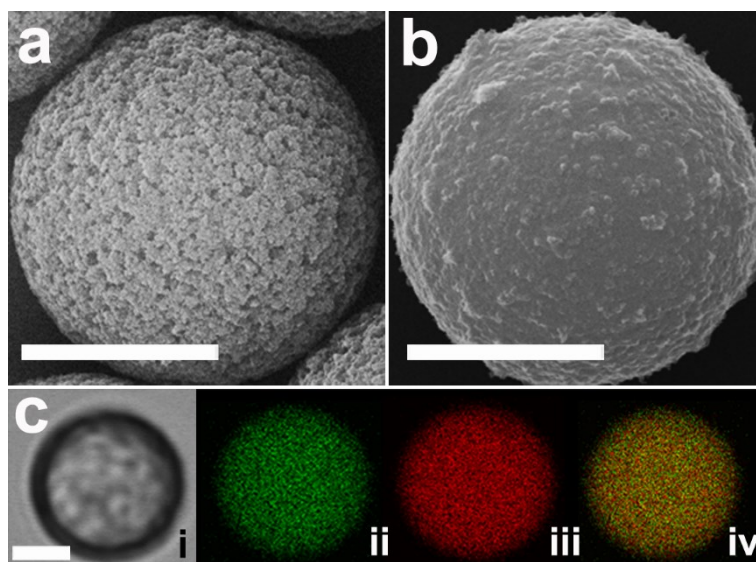


Figure S9. Representative SEM images of (a) original MPSBs-5.5 and (b) dual dyes doped MPSBs-5.5 FEMs at high magnification. (c) Confocal images of dual dyes doped MPSBs-5.5 FEMs taken in (i) bright field, (ii) channel 1 (515 ± 15 nm) for FITC, (iii) channel 2 (585 ± 15 nm) for RITC, and (iv) the merged one of channel 1 and channel 2. Scale bar, (a, b) $3 \mu\text{m}$, (c) $2 \mu\text{m}$.

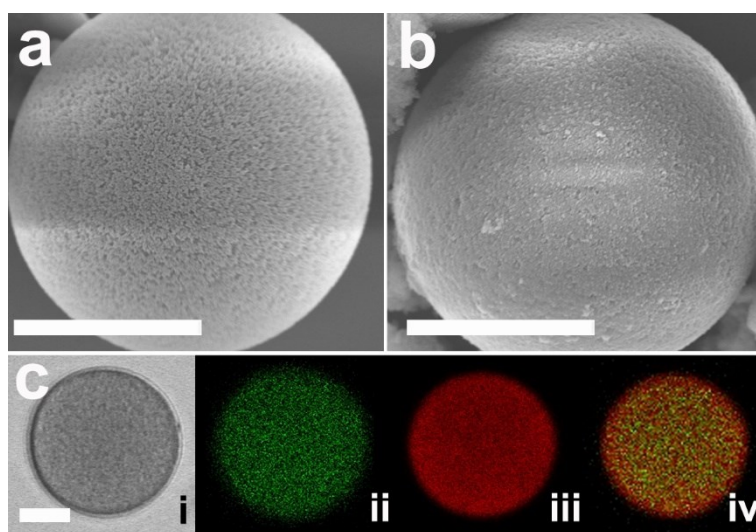


Figure S10. Representative SEM images of (a) original MPMBs-18.4 and (b) dual dyes doped MPMBs-18.4 FEMs at high magnification. (c) Confocal images of dual dyes doped MPMBs-18.4 FEMs taken in (i) bright field, (ii) channel 1 (515 ± 15 nm) for FITC, (iii) channel 2 (585 ± 15 nm) for RITC, and (iv) the merged one of channel 1 and channel 2. Scale bar, (a, b) $10 \mu\text{m}$, (c) $6 \mu\text{m}$.

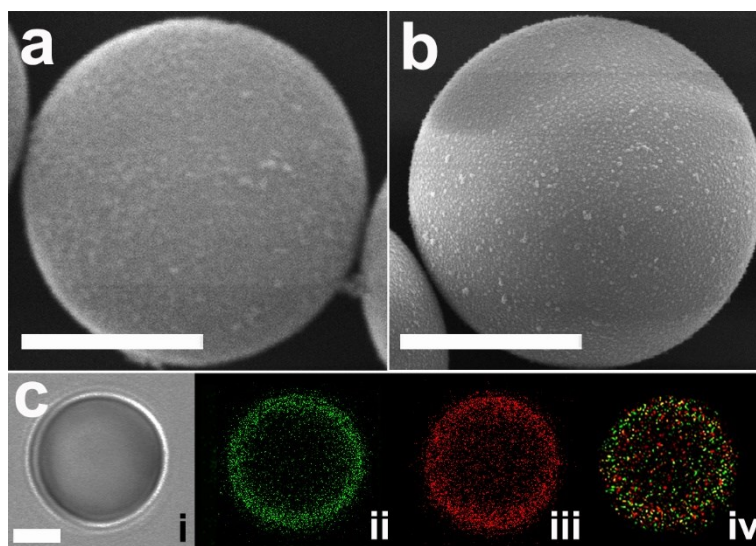


Figure S11. Representative SEM images of (a) original SPSBs-5.8 and (b) dual dyes doped SPSBs-5.8 FEMs at high magnification. (c) Confocal images of dual dyes doped SPSBs-5.8 FEMs taken in (i) bright field, (ii) channel 1 (515 ± 15 nm) for FITC, (iii) channel 2 (585 ± 15 nm) for RITC, and (iv) the merged one of channel 1 and channel 2. Scale bar, (a, b) $3 \mu\text{m}$, (c) $2 \mu\text{m}$.

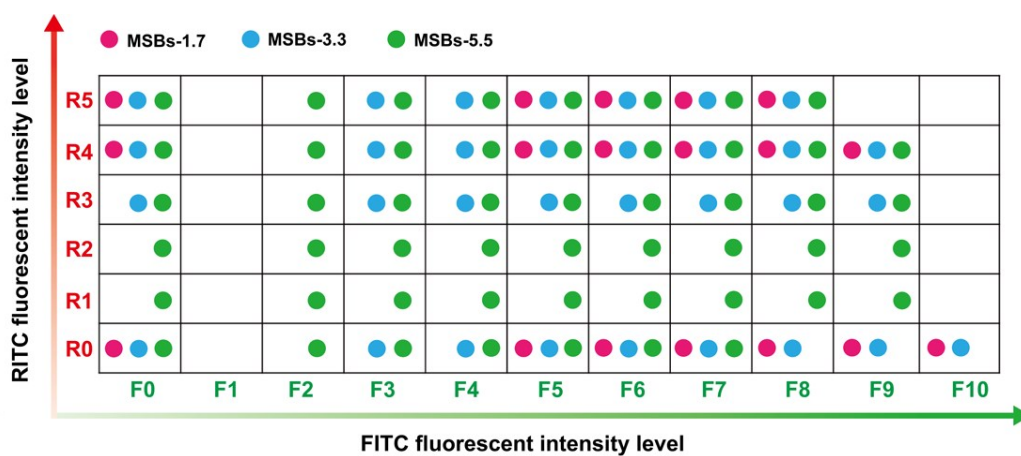


Figure S12. Encoding formula of dual dyes doped FEMs in FITC and RITC fluorescent intensity levels for different sized MSBs. The detailed formula of F0-F10 (FITC) and R0-R5 (RITC) is the same as that in Table S2.

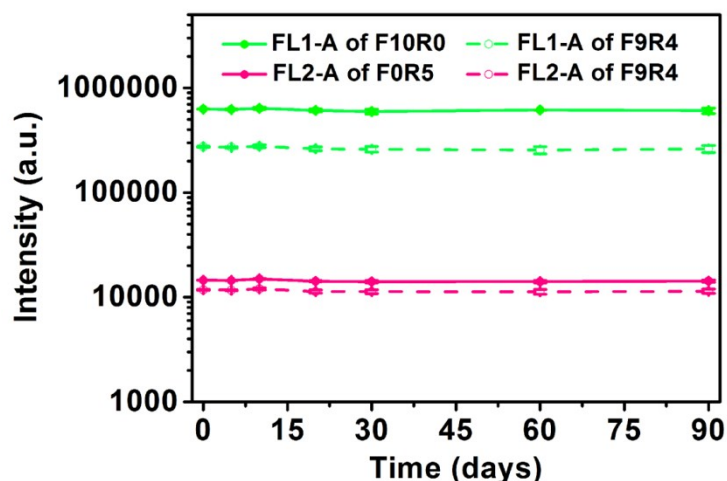


Figure S13. Fluorescence stability of F10R0, F0R5 and F9R4 MSBs-3.3 FEMs in aqueous solution measured via flow cytometry in FL1 (515 ± 10 nm) and FL2 (565 ± 10 nm) channels.

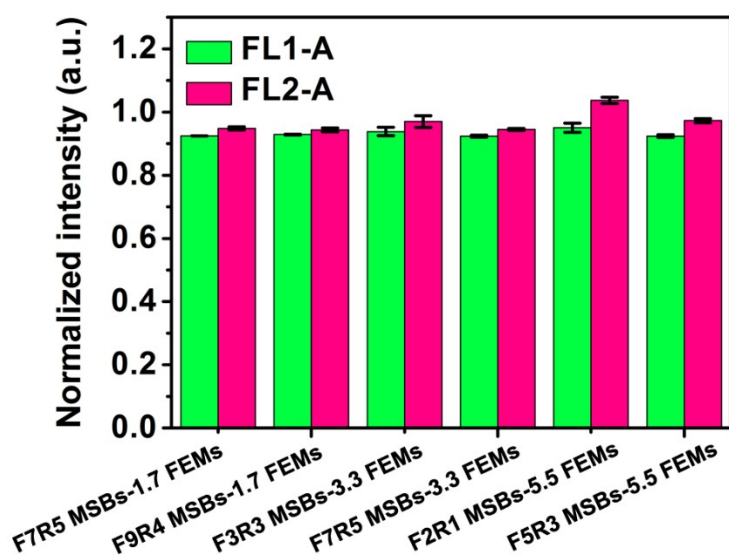


Figure S14. Tolerance stability of six typical FEMs analyzed via their normalized intensity of FL1 (515 ± 10 nm) and FL2 (565 ± 10 nm) in flow cytometry after undergoing a biodetection procedure when compared with their original fluorescence. A mixture containing 6×10^3 of each FEMs were dispersed in a 100 μ L of reaction system including 35 μ L of human serum and 65 μ L of PBST (10 mM, pH = 7.4), and then rotationally incubated at 37 $^{\circ}$ C for 1 h.

References

1. D. S.-z. Zhang, Y. Jiang, D. Wei, X. Wei, H. Xu and H. Gu, *Nanoscale*, 2018, **10**, 12461-12471.
2. M. Ankerst, M. M. Breunig, H.-P. Kriegel and J. Sander, *ACM Sigmod Rec.*, 1999, **28**, 49-60.